

Discrete Newtonian dynamics with Nosé-Hoover thermostats

Søren Toxvaerd

*Department of Science and Environment,
Roskilde University, Postbox 260, DK-4000 Roskilde**

Abstract

Almost all Molecular Dynamics (MD) simulations are discrete dynamics with Newton's algorithm first published in 1687, and much later by L. Verlet in 1967. Discrete Newtonian dynamics has the same qualities as Newton's classical analytic dynamics. Verlet also published a first-order expression for the instant temperature which is inaccurate but presumably used in most MD simulations. One of the motivations for the present article is to correct this unnecessary inaccuracy in *NVT* MD dynamics. Another motivation is to derive simple algorithms for the Nosé-Hoover *NVT* dynamics (NH) with the correct temperature constraint. The simulations with NH discrete Newtonian dynamics show that the NH works excellent for a wide range of the response time τ of the NH thermostat, but NH simulations favor a choice of a short response time, even shorter than the discrete time increment δt used in MD, to avoid large oscillations of the temperature.

* st@ruc.dk

I. INTRODUCTION

Newton published PHILOSOPHIÆ NATURALIS PRINCIPIA MATHEMATICA (*Principia*) in 1687 [1, 2] and he began *Principia* by postulating the discrete Newtonian dynamics in *Proposition I*, where he used the algorithm for discrete dynamics to derive his second law for classical mechanics. The classical analytic dynamics of N interacting objects is the exact solution, obtained by solving the coupled second-order analytic differential equations for the accelerations of the objects. The exact analytic solution for the dynamical evolution of the positions of the objects is characterized by being time-reversible and symplectic, and by having three invariances for a conservative system: the conservation of momentum, angular momentum, and the energy of the system. But Newton's discrete dynamics is also time reversible and symplectic and has the same three invariances [2], and if the exactness of classical mechanics is given by these five qualities, then his discrete dynamics is also exact. Furthermore, there exists a shadow Hamiltonian where discrete positions are located on the analytical trajectories for the shadow Hamiltonian [2–4]. This means that there is no qualitative difference between Newton's analytic and discrete dynamics.

The discrete Newtonian algorithm was much later in 1967 rediscovered by Loop Verlet [5] and used in his pioneering Molecular Dynamics (MD) simulation of a system of Lennard-Jones particles. The algorithm has been reformulated several times and appears under a variety of names, the most well-known is the Leapfrog version. Almost all MD simulations today in Natural Science are performed by Newton's discrete algorithm. A review of the discrete Newtonian dynamics is given in reference No.2 [2] with the proofs of the invariances for a conservative system. The proof of the conservation of the energy is also given here in the appendix.

Loop Verlet also derived a first-order expression $\mathbf{v}_{0,i}(t)$ for the discrete velocity $\mathbf{v}_i(t)$ for object No. i at time t obtained by a symmetric Taylor expansion [6]

$$\mathbf{v}_i(t) = \mathbf{v}_{0,i}(t) - \frac{1}{6} \frac{\delta t^2}{m_i} \mathbf{f}'_i(t) + \mathcal{O}(\delta t^4 \mathbf{f}''_i(t)) \quad (1)$$

with

$$\mathbf{v}_{0,i}(t) = \frac{\mathbf{r}_i(t + \delta t) - \mathbf{r}_i(t - \delta t)}{2\delta t} \quad (2)$$

from its positions $\mathbf{r}_i(t - \delta t)$ and $\mathbf{r}_i(t + \delta t)$, and this expression is used in today's MD [7, 8]. The velocity $\mathbf{v}_{0,i}(t)$ in Eq. (2) is the first term for the velocity in Verlet's forward and

backward Taylor expansion of the discrete position $\mathbf{r}(t)$, and if the velocity is approximated by this expression, it entails a systematic and sometimes significant error in the calculated temperature and in the heat capacity of a system [9]. It is the one of the reasons for this article, where the correct expression for the velocity and the kinetic energy is used to revise the formulation of the *NVT* Nosé-Hoover algorithm (NH) for *NVT* simulations [10]. Constant temperature MD has been simulated for many decades and the method is reviewed in [11]. Many of the algorithms for discrete dynamics at constant temperatures are, however, with broken time symmetry and irreversible dynamics. However, the NH dynamics, which is derived from the steady state Liouville equation for an extended phase space with friction with a friction coefficient $\eta(t)$, is time reversible [10, 12].

The article starts in Section 2 by presenting the expressions for the velocities, kinetic energy, and temperature by the use of the energy invariance derived in the appendix, and the NH algorithms for *NVT* discrete dynamics are presented in Section 3. The algorithms are used in Section 4 to obtain *NVT* state points for a system of Lennard-Jones particles (LJ). Section 5 summarizes the results.

II. DISCRETE NEWTONIAN DYNAMICS

The classical discrete dynamics between N spherically symmetrical objects with masses $m^N = m_1, m_2, ..m_i, .., m_N$ and positions $\mathbf{r}^N(t) = \mathbf{r}_1(t), \mathbf{r}_2(t), .., \mathbf{r}_i(t), .., \mathbf{r}_N(t)$ is obtained by Newton's discrete algorithm. Let the force, \mathbf{f}_i on object No. i be a sum of pairwise forces \mathbf{f}_{ij} between pairs of objects i and j

$$\mathbf{f}_i = \sum_{j \neq i}^N \mathbf{f}_{ij}. \quad (3)$$

Newton's discrete algorithm is a symmetrical time-centered difference whereby the dynamics is time reversible and symplectic. The Verlet formulation of the algorithm is

$$\mathbf{r}_i(t + \delta t) = 2\mathbf{r}_i(t) - \mathbf{r}_i(t - \delta t) + \frac{\delta t^2}{m_i} \mathbf{f}_i(i). \quad (4)$$

The energy in analytic dynamics is the sum of potential energy $U(\mathbf{r}^N(t))$ and kinetic energy $K(t)$, and it is an invariance for a conservative system with analytic dynamics. There is, however, a problem with the determination of the kinetic energy in the discrete dynamics since the velocities at time t are not known. Traditionally one uses Eq. (2) and

the expressions

$$K_0(t) = \sum_i^N \frac{1}{2} m_i \mathbf{v}_{0,i}(t)^2 \quad (5)$$

$$E_0(t) = U(\mathbf{r}^N(t)) + K_0(t) \quad (6)$$

for the velocity, kinetic energy $K(t)$, potential energy $U(\mathbf{r}^N(t))$ and energy $E(t)$ in MD. But the total energy E_0 obtained by using Eq. (6) with $K(t) = K_0(t)$ for the kinetic energy fluctuates with time although it remains constant, averaged over long time intervals. This is due to the fundamental quality of Newton's discrete dynamics, where the positions and momenta appear asynchronous and with a discrete change in momentum at time t . The energy invariance in discrete Newtonian dynamics (D) is derived in the appendix. The kinetic energy $K_D(t)$ in the time interval $[t - \delta t/2, t + \delta t/2]$ is

$$\begin{aligned} K_D &= \frac{1}{2}(K_{D+} + K_{D-}) = \\ &= \frac{1}{2} \sum_i^N \frac{1}{2} m_i \left[\frac{(\mathbf{r}_i(t + \delta t) - \mathbf{r}_i(t))^2}{\delta t^2} + \frac{(\mathbf{r}_i(t) - \mathbf{r}_i(t - \delta t))^2}{\delta t^2} \right] \\ &= \frac{1}{2} \sum_i^N \frac{1}{2} m_i (\mathbf{v}_i(t + \delta t/2)^2 + \mathbf{v}_i(t - \delta t/2)^2). \end{aligned} \quad (7)$$

A. The temperature in discrete Newtonian dynamics

The constant kinetic energies in the time intervals $[t - \delta t/2, t]$ and $[t, t + \delta t/2]$ in between a force impulse at time t are related [13]. It is easy to derive the relation

$$\mathbf{v}_{0,i}(t)^2 = \frac{1}{2} \mathbf{v}_i(t + \delta t/2)^2 + \frac{1}{2} \mathbf{v}_i(t - \delta t/2)^2 - \frac{1}{4} (\delta t / m_i \mathbf{f}_i(t))^2 \quad (8)$$

from Eq. (4) between the first-order expression Eq. (2) for the square of the velocity at time t and the well-defined expression for the square of the velocities $\mathbf{v}_i(t - \delta t/2)$ and $\mathbf{v}_i(t + \delta t/2)$ in the time intervals $[t - \delta t/2, t]$ and $[t, t + \delta t/2]$. The corresponding expression for the kinetic energy, $K_0(t)$, and the traditional value for the temperature used in MD simulations

$$k_B T_0(t) = \frac{\langle 2K_0(t) \rangle}{N_f} \quad (9)$$

used in MD simulations for a system with N_f degrees of freedom is less than the mean kinetic energy, $K_D(t)$, and the temperature

$$k_B T_D(t) = \frac{\langle 2K_D(t) \rangle}{N_f}. \quad (10)$$

In the discrete time interval $[t - \delta t/2, t + \delta t/2]$ the relation is

$$K_0(t) = K_D(t) - \sum_i^N \frac{1}{8} \delta t^2 / m_i \mathbf{f}_i(t)^2. \quad (11)$$

The correct temperature T_D is bigger than T_0 and the difference between T_D and T_0 increases with density, temperature, and the discrete time step δt . The difference is relatively small and of the order of a few percent at state points with low pressure, but it is significant for state points with high densities, pressure, temperatures, the strength of the repulsive forces, or for large time increments δt [9].

III. *NVT* ENSEMBLE SIMULATIONS WITH THE NOSÉ-HOOVER THERMOSTATS

Many *NVT* ensemble simulations in MD are with the Nosé-Hoover thermostat (NH-MD) where a friction $\eta(t)\mathbf{p}_i(t)$ acts simultaneously with the force $\mathbf{f}_i(t)$ [10]. The Hamilton formulation of classical dynamics with the friction is [10, 12]

$$\dot{\mathbf{r}}_i(t) = \mathbf{p}_i(t) \quad (12)$$

$$\dot{\mathbf{p}}_i(t) = \mathbf{f}_i(t)/m_i - \eta(t)\mathbf{p}_i(t) \quad (13)$$

$$\dot{\eta}(t) = \alpha^{-1}(K(t) - K), \quad (14)$$

with a restoring friction $\eta(t)\mathbf{p}_i(t)$ which constrains the kinetic energy $K(t)$ to $K = 2N_f k_B T$. The damping factor α is expressed as

$$\alpha = N_f \tau / 2, \quad (15)$$

where τ is a characteristic "response" time of the thermostat [14].

The discrete Newtonian dynamics with the time symmetrical Leapfrog formulation with NH-MD is

$$\mathbf{r}_i(t + \delta t) = \mathbf{r}_i(t) + \delta t \mathbf{v}_i(t + \delta t/2) \quad (16)$$

$$\begin{aligned} \mathbf{v}_i(t + \delta t/2) &= \mathbf{v}_i(t - \delta t/2) + \delta t / m_i \mathbf{f}_i(t) \\ &\quad - \eta(t)(\mathbf{v}_i(t + \delta t/2) + \mathbf{v}_i(t - \delta t/2))/2, \end{aligned} \quad (17)$$

and the discrete friction variable $\eta(t)$ can either be updated from two sets of discrete values $\eta(t - \delta t), \eta(t)$ by

$$\eta(t + \delta t) = \eta(t - \delta t) + \delta t / \tau (T_D(t) - T) \text{ Method I}, \quad (18)$$

or by

$$\eta(t + \delta t) = \eta(t) + \delta t/\tau(T_{D_+}(t) - T) \text{ Method II,} \quad (19)$$

where $k_B T_{D_+} = \sum_i^N m_i \mathbf{v}(t + \delta t/2)^2/N_f$. Eq. (18) is the time centred analog to Newton's discrete central difference algorithm. The time symmetry and time reversibility is maintained in the NH-MD discrete dynamics with both methods, and both methods have been used in NH-MD [14, 15].

The NH dynamics can be extended to include more than one thermostat and this has been used in simulations of systems with organic chain molecules. The thermostats can equilibrate specific modes in the systems or act on all N_f degrees of freedom [16]. In the present formulation of NH dynamics and with n thermostats which act with all N_f modes

$$\begin{aligned} \eta_1(t + \delta t) &= \eta_1(t - \delta t) + \delta t/\tau_1(T_D(t) - T) \\ \eta_2(t + \delta t) &= \eta_2(t - \delta t) + \delta t/\tau_2(T_D(t) - T) \\ &\dots\dots\dots, \end{aligned} \quad (20)$$

and with a total friction $\eta = \sum_i^n \eta_i/n$.

Eq. (17) can be rearranged to

$$\mathbf{v}_i(t + \delta t/2) = \frac{\mathbf{v}_i(t - \delta t/2)(1 - \eta(t)/2) + \delta t/m_i \mathbf{f}_i(t)}{1 + \eta(t)/2}, \quad (21)$$

and the NVT time reversible NH-MD dynamics is obtained by the NH-MD algorithm: Eqn. (16) and (21) with either Eq. (18), and/or Eq. (19), and/or Eq. (20).

IV. NVT SIMULATIONS

The Nosé-Hoover friction $\eta(t)$ thermostats the system's instantaneous kinetic energy and temperature $T(t)$ using kinetic energy, Eq. (18) or Eq.(19). Most NVT_0 simulations with NH-MD use Verlet's expression $T_0(t)$, Eq. (9), for the temperature. The exact expression for the kinetic energy and the instant temperature $T_D(t)$ by the discrete dynamics is, however systematically higher and given by Eq. (10). The difference between the two canonical simulations, NVT_0 , and NVT_D , increases with the discrete time increment δt and the force according to Eq. (8). It is of the order a few percent or less for many MD NVE simulations at moderate densities and force fields [9], but can be much larger for stronger forces.

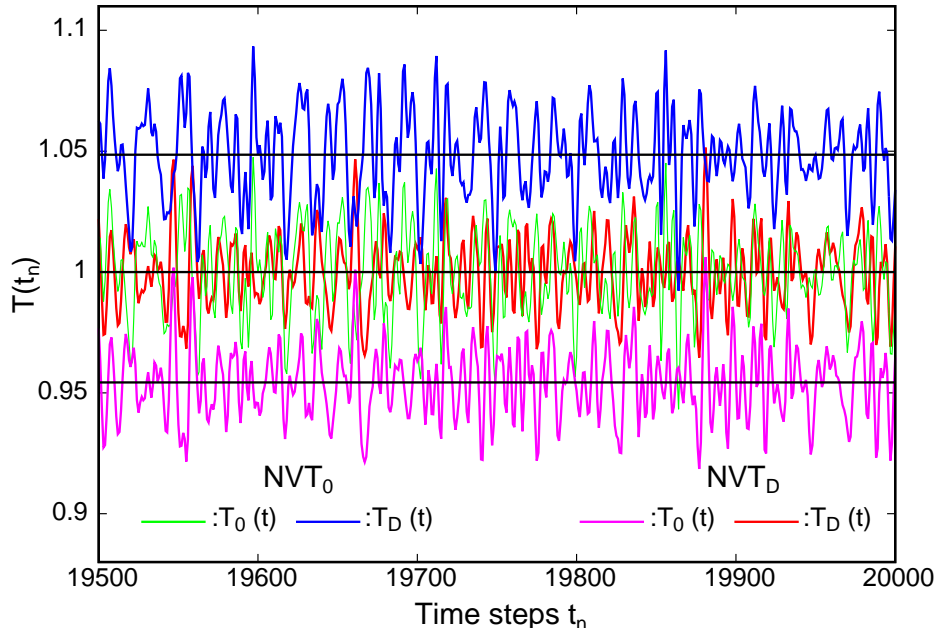


FIG. 1: NH-MD with $T_{Thermostat} = T_0 = 1.00$ (NVT_0 , old NH-MD), and with $T_{Thermostat} = T_D = 1.00$ (NVT_D , present NH-MD). The figure shows five hundred (representative) time steps for the simulations of 10^6 time steps. The temperatures \bar{T}_D and the root mean square (rms) fluctuations are given in Table I.

The differences between the two ensemble simulations, NVT_0 and NVT_D , where the instant temperature is either given by $T_0(t)$ or by $T_D(t)$, are determined for a Lennard-Jones system (LJ). The Lennard-Jones system is a simple model of a system with the classical gas-liquid-solid thermodynamic behavior. Systems of $N = 2000$ LJ particles were simulated for various state points ρ, T . The differences between NVT_0 and NVT_D at the high density $[\rho = 1.40, T = 1.00]$ fluid state point, and with $\delta t = 0.010$ and $\tau = 0.0010$ [17] are shown in Figure 1. The NH thermostat constrains a specified kinetic energy either to a given temperature T by Eq. (9): NVT_0 with $T_0(t) = T$, or by Eq. (10): NVT_D with $T_D(t) = T$. The mean canonical temperatures \bar{T}_0 and \bar{T}_D , respectively, are in both cases equal to the input temperature $T = 1$, and in both cases the difference between NVT_0 and NVT_D , obtained from 10^6 time steps are ≈ 4 - 5 per cent. For NVT_0 : $T_0 = 1.0000000$, green curve in Figure 1; $T_D = 1.049$, blue curve. For NVT_D : $T_D = 1.0000000$, red curve in Figure 1; $T_0 = 0.954$, magenta curve. (The figure shows the difference in a short time interval of five hundred steps).

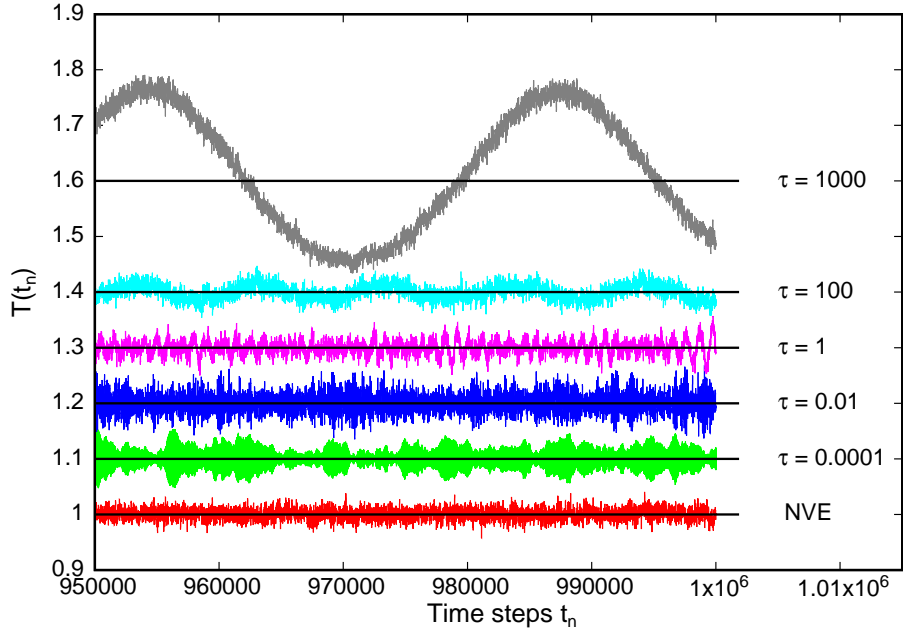


FIG. 2: Five evolutions of $T_D(t)$ in a LJ system of $N = 2000$ particles with $\delta t = 0.005$ and with a NH thermostat with $T = 1.0$ (Method I, Eq. (18)) together with the corresponding temperature without a thermostat (NVE). (Four NH-evolutions are parallel shifted with succeeding $\Delta T = 0.1$, and the last evolution with $\tau = 1000$ is shifted with $\Delta T = 0.2$.) All six simulations are started from the same NVE start configuration with different values of τ . The figure shows the last 50000 time steps for the simulations of 10^6 time steps. The temperatures \bar{T}_D and the root mean square (rms) fluctuations are given in Table I.

A. Nosé-Hoover simulations of a Lennard-Jones system

The two NH algorithms for NVT dynamics (I and II) are tested by MD simulations of a LJ system with the thermostats at various state points in the fluid state of the LJ system. The first examples are for a liquid state point $(T, \rho) = (1, 0.60)$ near the coexisting liquid with the density $\rho_l = 0.589$ at $T = 1.00$ [18]. The temperatures $T_D(t)$ for various values of the NH-response time τ are shown in Figure 2, and the mean temperatures and their root mean fluctuations are given in Table I. The thermostats work excellent for a wide range of the values of the response time τ but the system's instant temperature $T_D(t)$ exhibits oscillations for values of the response time $\tau \gg 1$, whereas the thermostat works excellent for smaller values, and even for response times $\tau < \delta t$.

TABLE I: Temperatures in the LJ system.

τ	$T_D \pm rms$	$T_0 \pm rms$	$\eta \pm rms$	Method
-	$1.000000000 \pm 9.5 \times 10^{-3}$	-	NVE	
0.0001	$0.999999993 \pm 1.7 \times 10^{-2}$	$0.999014 \pm 1.7 \times 10^{-2}$	$-2.06 \times 10^{-6} \pm 0.18$	I
0.0001	$1.000000025 \pm 1.8 \times 10^{-2}$	$0.999023 \pm 1.8 \times 10^{-2}$	$1.7 \times 10^{-6} \pm 1.4 \times 10^{-2}$	II
0.001	$1.000000970 \pm 1.7 \times 10^{-2}$	$0.999025 \pm 1.7 \times 10^{-2}$	$-2.81 \times 10^{-6} \pm 2.1 \times 10^{-3}$	I
0.01	$1.000000052 \pm 1.8 \times 10^{-2}$	$0.999024 \pm 1.8 \times 10^{-2}$	$2.39 \times 10^{-6} \pm 2.1 \times 0.1277$	I
0.1	$0.999998637 \pm 1.8 \times 10^{-2}$	$0.999023 \pm 1.8 \times 10^{-2}$	$-1.68 \times 10^{-6} \pm 4.0 \times 10^{-2}$	I
1	$1.000005194 \pm 1.8 \times 10^{-2}$	$0.999030 \pm 1.8 \times 10^{-2}$	$3.76 \times 10^{-7} \pm 1.3 \times 10^{-2}$	I
1	$0.999995501 \pm 1.9 \times 10^{-2}$	$0.999029 \pm 1.9 \times 10^{-2}$	$-9.16 \times 10^{-7} \pm 3.2 \times 10^{-3}$	II
10	$0.999986336 \pm 1.9 \times 10^{-2}$	$0.999011 \pm 1.7 \times 10^{-2}$	$1.29 \times 10^{-6} \pm 4.3 \times 10^{-3}$	I
100	$0.999883749 \pm 2.9 \times 10^{-2}$	$0.998908 \pm 2.9 \times 10^{-2}$	$2.3 \times 10^{-6} \pm 2.3 \times 10^{-3}$	I
1000	0.999458904 ± 0.12108	0.998477 ± 0.12083	$1.73 \times 10^{-5} \pm 3.2 \times 10^{-3}$	I
1000	0.999516366 ± 0.1236		$1.50 \times 10^{-5} \pm 3.2 \times 10^{-3}$	II

Table I contains also data for NH dynamics with Method II for $\tau = 0.0001, 1$ and 1000 , respectively, and there are no differences between the mean temperatures obtained by the two algorithms. The thermostats were tested for different temperatures and densities, including a fluid system at the high density $\rho = 1.40$ and the NH dynamics work excellently for both methods. The table for the NVT_D with $T_D = 1.00$ also lists the mean values \bar{T}_0 . They deviate marginally from \bar{T}_D at this state point with pressure $P \approx 0$ near a liquid in coexisting with gas where the LJ particles are near the minimum potential energy state, and where the forces are ≈ 0 .

The instant temperature $T_D(t)$ with NVT_D dynamics, and for the smallest value of $\tau = 0.0001$ is shown in green in Figure 2. The temperatures exhibit some "zones" with different amplitudes of the fluctuations. The observed "zones" with a single thermostat friction can be caused by a nonergodicity of the NH-dynamics, and it can be removed by an additional friction [19]. The simulations of the LJ system at $T, \rho = 1, 0.6$ with two independent NH thermostats are shown in Figure 3. The fluctuation zones are removed by the use of two independent thermostats. However, extended investigations of NH-MD of systems with this nonergodicity show, that there are systems for which it is not possible to

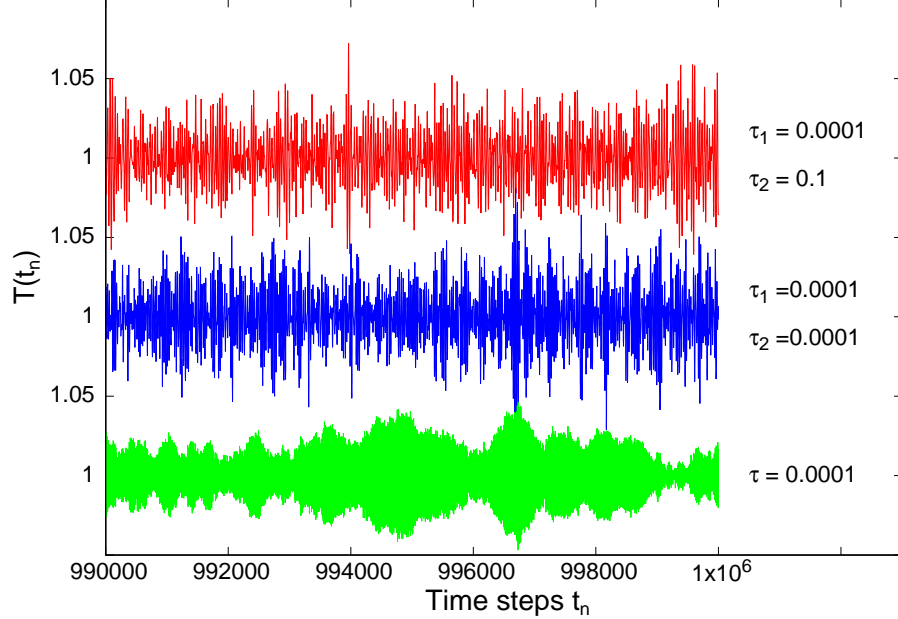


FIG. 3: The temperature fluctuations of $T_D(t)$ in the temperature interval $[0.95, 1.05]$ for NH-dynamics with one and with two thermostats. The fluctuations of the temperature with one thermostat and $\tau = 0.0001$ are also shown in green in Figure 1. The fluctuations in the temperature interval $[0.95, 1.05]$ with two thermostats are shown above, and for two sets of frictions. With red is for $\tau_1 = 0.0001$ and $\tau_2 = 0.1$. With blue is $T_D(t)$ with $\tau_1 = \tau_2 = 0.0001$ with different start values of $\eta_1(0), \eta_1(-\delta t)$ and $\eta_2(0), \eta_2(-\delta t)$, respectively.

achieve ergodicity within computationally achievable time by the use of two NH thermostats [20].

A typical situation in NH-MD is a calibration of a system from a temperature $T_D(0) = T_1$ to another temperature T_2 . The temperature evolution in the NH thermostated LJ system by changing the thermostat temperature from $T_1 = 1.00$ to $T_2 = 2.00$ is shown in Figure 4 for two different values of the response time τ . With blue is $T_D(t)$ for a relative long response time $\tau = 1.00$ and with red is for a short response time $\tau = 0.0001$. The instant temperature oscillates in both cases around the new target temperature $T_2 = 2.00$, but the system with the short response time converges rapidly to instant temperatures near T_2 whereas the temperature oscillates with large amplitudes for many thousand time steps in the case with a long response time. The lower inset shows the evolution shortly after

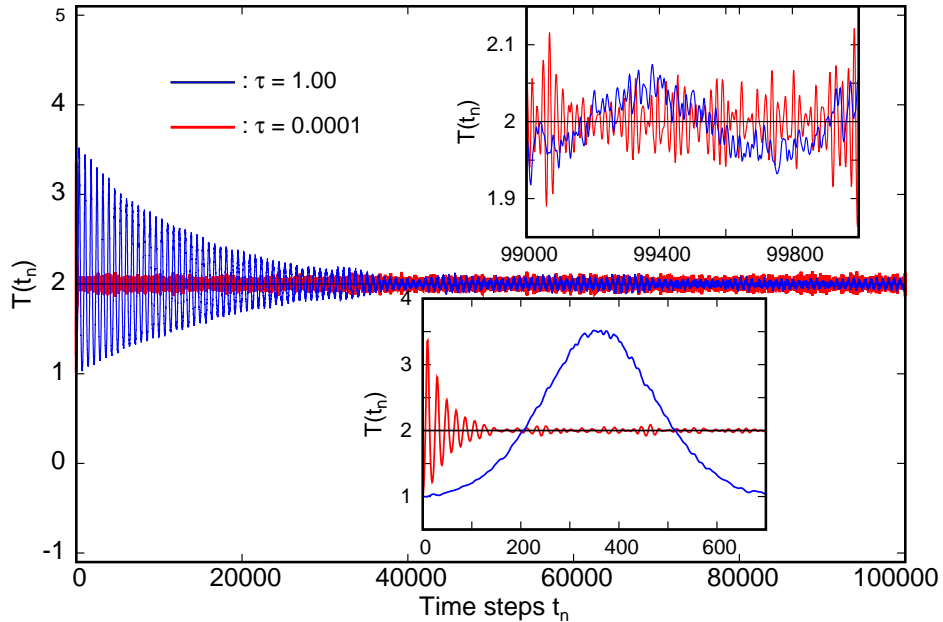


FIG. 4: Temperature evolution in the LJ system by changing the thermostat temperature from $T_1 = 1.00$ to $T_2 = 2.00$. With blue is $T_D(t)$ for a relative long response time $\tau = 1.00$ and with red is for a short response time $\tau = 0.0001$. The lower inset shows the temperature evolution at the start of the calibration and the upper inset is at the end of the calibration of the temperature.

the start of the calibration and the upper inset are for the temperatures after \approx hundred thousand time steps.

V. SUMMARY

Almost all MD simulations are with Newtonian discrete dynamics with Newton's Verlet or the equivalent Leapfrog algorithm, and the discrete Newtonian dynamics has the same qualities as Newton's classical analytic dynamics [2]. Verlet also proposed an approximative expression, Eq. (2), for the temperature at t_n after n time steps [5], which presumably is used in most MD simulations, but the first-order expression is not useful at positions where an object is exposed to a strong force e.g. at an elastic collision. The expression for the velocity at the discrete dynamics has been improved by including higher order terms in the Taylor expansion, Eq. (1), by a spline fit to the discrete positions, or by using a higher-order

predictor-corrector algorithm. A. Rahman used a higher-order predictor-corrector algorithm in the very first MD simulation [21], and also the Runge-Kutta algorithm is occasionally used in *NVT* MD dynamics [22]. But almost all *NVT* dynamics are with Newton's discrete algorithm, a thermostat, and by using Eq. (2) for the velocity at t_n .

The approximative expressions for the velocity and kinetic energy at the time step t_n can be replaced by the exact expressions for velocities and kinetic energies in the time intervals at t_n . One of the motivations for the present article is to correct this unnecessary error in the determination of the temperature in Newton's discrete dynamics. Another motivation is to derive simple algorithms for the Nosé-Hoover *NVT* dynamics with the correct kinetic constraint on the discrete Newtonian dynamics.

The simulations with NH-MD discrete Newtonian dynamics show that NH-MD works excellent for a wide range of the response time τ , but the NH-MD favor a choice of a short response time, even shorter than the discrete time increment δt in the MD, in order to avoid large oscillations of the temperature.

VI. APPENDIX

The energy invariance

The energy invariance, E_D in Newton's discrete dynamics (D) can be seen by considering the change in kinetic energy, δK_D , potential energy, δU_D , and the work, W_D done by the force in the time interval $[t - \delta t/2, t + \delta t/2]$. The loss in potential energy, $-\delta U_D$ is defined as the work done by the forces at a move of the positions [23]. An expression for the work, W_D done in the time interval by the discrete dynamics from the position $(\mathbf{r}_i(t) + (\mathbf{r}_i(t - \delta t)))/2$ at $t - \delta t/2$ to the position $(\mathbf{r}_i(t + \delta t) + \mathbf{r}_i(t))/2$ at $t + \delta t/2$ with the change in position $(\mathbf{r}_i(t + \delta t) - \mathbf{r}_i(t - \delta t))/2$ is [2]

$$-\delta U_D = W_D = \sum_i^N \mathbf{f}_i(t) (\mathbf{r}_i(t + \delta t) - \mathbf{r}_i(t - \delta t))/2. \quad (22)$$

By rewriting Eq. (4) to

$$\mathbf{r}_i(t + \delta t) - \mathbf{r}_i(t - \delta t) = 2(\mathbf{r}_i(t) - \mathbf{r}_i(t - \delta t)) + \frac{\delta t^2}{m_i} \mathbf{f}_i(t), \quad (23)$$

and inserting in Eq. (22) one obtains an expression for the total work in the time interval

$$-\delta U_D = W_D = \sum_i^N [(\mathbf{r}_i(t) - \mathbf{r}_i(t - \delta t)) \mathbf{f}_i(t) + \frac{\delta t^2}{2m_i} \mathbf{f}_i^2]. \quad (24)$$

An expression for the mean kinetic energy K_D of the discrete dynamics in the time interval $[t - \delta t/2, t + \delta t/2]$ is

$$\begin{aligned}
K_D &= K_{D+} + K_{D-} = \\
&= \frac{1}{2} \sum_i^N \frac{1}{2} m_i \left[\frac{(\mathbf{r}_i(t + \delta t/2) - \mathbf{r}_i(t))^2}{\delta(t/2)^2} + \frac{(\mathbf{r}_i(t) - \mathbf{r}_i(t - \delta t/2))^2}{\delta(t/2)^2} \right] \\
&= \frac{1}{2} \sum_i^N \frac{1}{2} m_i \left[\frac{(\mathbf{r}_i(t + \delta t) - \mathbf{r}_i(t))^2}{\delta t^2} + \frac{(\mathbf{r}_i(t) - \mathbf{r}_i(t - \delta t))^2}{\delta t^2} \right].
\end{aligned} \tag{25}$$

, and with the change in the time interval

$$\begin{aligned}
\delta K_D &= K_{D+} - K_{D-} \\
&= \sum_i^N \frac{1}{2} m_i \left[\frac{(\mathbf{r}_i(t + \delta t) - \mathbf{r}_i(t))^2}{\delta t^2} - \frac{(\mathbf{r}_i(t) - \mathbf{r}_i(t - \delta t))^2}{\delta t^2} \right].
\end{aligned} \tag{26}$$

,

By rewriting Eq. (4) to

$$\mathbf{r}_i(t + \delta t) - \mathbf{r}_i(t) = \mathbf{r}_i(t) - \mathbf{r}_i(t - \delta t) + \frac{\delta t^2}{m_i} \mathbf{f}_i(t) \tag{27}$$

and inserting the squared expression for $\mathbf{r}_i(t + \delta t) - \mathbf{r}_i(t)$ in Eq. (25), the change in kinetic energy is

$$\delta K_D = \sum_i^N \left[(\mathbf{r}_i(t) - \mathbf{r}_i(t - \delta t)) \mathbf{f}_i(t) + \frac{\delta t^2}{2m_i} \mathbf{f}_i(t)^2 \right]. \tag{28}$$

The energy invariance in Newton's discrete dynamics is expressed by Eqn. (24), and Eq. (28) as [2]

$$\delta E_D = \delta U_D + \delta K_D = 0. \tag{29}$$

ACKNOWLEDGEMENTS

The cooperation over many years with my dear friend Luis F. Rull is gratefully acknowledged.

[1] Newton, I., 1687, *PHILOSOPHIAE NATURALIS PRINCIPIA MATHEMATICA. LONDINI, Anno MDCLXXXVII.*

- [2] Toxvaerd, S., 2023, *Comprehensive Computational Chemistry* **3**, 329 (Elsevier, Amsterdam, 2023).
- [3] Toxvaerd, S. 1994 Phys. Rev. E, **50**, 2271 .
- [4] Toxvaerd, S., Heilmann, O. J., and J. Dyre, J. C., 2012 *J. Chem. Phys.* **136**, 224106.
- [5] Verlet, L., 1967, *Phys. Rev.*, **159**, 98.
- [6] See Reference No. 2, Appendix.
- [7] Allen, M. P., Tildesley, D. J., 1987, *Computer Simulation of Liquids* (Oxford Science Publications, Oxford, 1987).
- [8] D. Frenkel, D., Smit, B., 2023, *Understanding Molecular Simulation* (Academic, New York, 2023).
- [9] Toxvaerd, S., 2024, *Phys. Rev. E*, *in press*.
- [10] Hoover, W. G., 1985, *Phys. Rev. A*, **31**, 1695.
- [11] Harish M. S., and Patra P. K., 2021, *Mol. Phys.*, **47**, 701.
- [12] Hoover, W. G., 1991, *Computational Statistical Mechanics* (Elsevier, Amsterdam, 1991).
- [13] Toxvaerd, S., 2013, *J. Chem. Phys.*, **139**, 224106.
- [14] Toxvaerd, S., 1991, *Mol. Phys.*, **72**, 159.
- [15] Holian, B. L., De Groot, A. J., Hoover, W. G., and Hoover, C. G., 1990, *Phys. Rev. A*, **41**, 3592.
- [16] Frenkel, D., Smit, B., 2002, *Understanding Molecular Simulation* Chapter 6 and Appendix L, (Academic, New York, 2002). .
- [17] Units in MD of LJ systems: lengths in unit of σ , energy unit ϵ , time unit $t^* = \sigma\sqrt{m/\epsilon}$. Temperature is $k_B T/\epsilon$. The LJ forces are cutted and shifted at $r_{cut}/\sigma = 2.5$, for cut-and-shifted forces in MD: Toxvaerd, S., and Dyre, J. C., 2012, *J. Chem. Phys.* **134**, 081102.
- [18] Watanabe, H., Ito, N., and Hu, C-K., 2012, *J. Chem. Phys.*, **136**, 204102. *Mol. Phys.*, **87**, 1117.
- [19] Martyna, G. L., Klein, M., and Tuckerman, M., 1992, *J. Chem. Phys.*, **97**, 2635.
- [20] Patra, P. K., Bhattacharya, B., 2014, *Phys. Rev. E*, **90**, 043304.
- [21] Rahman, A., 1964, *Phys. Rev.*, **136**, A 405.
- [22] Janežič, D., and Orel, B., 1993, *J. Chem. Inf. Comput. Sci.*, **33**, 252.
- [23] Goldstein, H., 1980, *Classical Mechanics*,(Addison-Wesley Press Second Ed. 1980), Chap. 1.